Science of the Total Environment 502 (2015) 330–343

Contents lists available at ScienceDirect

Science of the Total Environment

journal homepage: www.elsevier.com/locate/scitotenv

Geochemical processes controlling water salinization in an irrigated basin in Spain: Identification of natural and anthropogenic influence

D. Merchán [a,*], L.F. Auqué [b], P. Acero [b], M.J. Gimeno [b], J. Causapé [a]

[a] Geological Survey of Spain — IGME, C/Manuel Lasala 44 9B, 50006 Zaragoza, Spain
[b] University of Zaragoza — Department of Earth Sciences (Geochemical Modelling Group), C/Pedro Cerbuna 12, 50009 Zaragoza, Spain

HIGHLIGHTS

- Salinization in Lerma Basin was controlled by the dissolution of soluble salts.
- Water salinization and nitrate pollution were found to be independent processes.
- High NO_3, fresh groundwater evolved to lower NO_3, higher salinity surface water.
- Inverse and direct geochemical modeling confirmed the hypotheses.
- Salinization was a natural ongoing process slightly enhanced by land use.

ARTICLE INFO

Article history:
Received 12 May 2014
Received in revised form 10 September 2014
Accepted 12 September 2014
Available online 28 September 2014

Editor: Eddy Y. Zeng

Keywords:
Mineral dissolution
Cation exchange reactions
Nitrate pollution
Multivariate analysis
Geochemical modeling

ABSTRACT

Salinization of water bodies represents a significant risk in water systems. The salinization of waters in a small irrigated hydrological basin is studied herein through an integrated hydrogeochemical study including multivariate statistical analyses and geochemical modeling. The study zone has two well differentiated geologic materials: (i) Quaternary sediments of low salinity and high permeability and (ii) Tertiary sediments of high salinity and very low permeability. In this work, soil samples were collected and leaching experiments conducted on them in the laboratory. In addition, water samples were collected from precipitation, irrigation, groundwater, spring and surface waters. The waters show an increase in salinity from precipitation and irrigation water to ground- and, finally, surface water. The enrichment in salinity is related to the dissolution of soluble mineral present mainly in the Tertiary materials. Cation exchange, precipitation of calcite and, probably, incongruent dissolution of dolomite, have been inferred from the hydrochemical data set. Multivariate statistical analysis provided information about the structure of the data, differentiating the group of surface waters from the groundwaters and the salinization from the nitrate pollution processes. The available information was included in geochemical models in which hypothesis of consistency and thermodynamic feasibility were checked. The assessment of the collected information pointed to a natural control on salinization processes in the Lerma Basin with minimal influence of anthropogenic factors.

1. Introduction

Salinization of water bodies represents a significant risk in water systems regarding suitability for irrigation (Tanji, 1990), other human uses (Peck and Hatton, 2003) or ecosystem health (Nielsen et al., 2003). There are many processes which can cause water salinization. For instance, the main sources of groundwater salinization in the US are natural saline groundwater, sea-water intrusion, halite dissolution, oil- and gas-field activities, saline seep, road salting and agricultural techniques (Richter and Kreitler, 1991).

Groundwater salinization by agricultural practices has been widely reported all around the world (e.g., Koh et al., 2007; Stigter et al., 2006; Yuce et al., 2006). Specifically, irrigated agriculture represents an enhanced pressure on the hydrological system receiving irrigation return flows, with in general higher salinization rates under irrigated areas in comparison with rainfed areas (Johansson et al., 2009). Some examples of the reported processes that increase water salinity include the recirculation of irrigation water (Stigter et al., 2006), the application of agrochemicals (Kume et al., 2007), or the enhanced weathering of existing materials in the area (Kim et al., 2005; Koh et al., 2007). In some cases, natural salinization processes of water bodies are enhanced by irrigated agriculture, either by the transport of solutes in the water (Johansson et al., 2009) or by the depletion of aquifers and consequent concentration of salts (Chaudhuri et al., 2014). Irrigated agriculture may

* Corresponding author.
E-mail addresses: d.merchan@igme.es, eremad@hotmail.com (D. Merchán).

http://dx.doi.org/10.1016/j.scitotenv.2014.09.041
0048-9697/

induce salinization not only in groundwater, but also in surface waters (e.g., Duncan et al., 2008; Isidoro et al., 2006). In any case, the interaction between ground and surface waters adds complexity to the behavior of these hydrological systems. However, salinization in irrigated areas may be related to natural ongoing processes which may be, to a certain degree, enhanced by the addition of irrigation water (Carreira et al., 2014; Chaudhuri and Ale, 2014; Isidoro et al., 2006; Tedeschi et al., 2001) or a direct consequence of the irrigation itself (Stigter et al., 2006), since the dominating salinization processes are very site-specific (Duncan et al., 2008). For instance, irrigation water enhances salinization processes in areas with available salts in the geological substrate, which are mobilized by the extra available water. In other cases, the continuous use of groundwater for irrigation may cause salinization due to the evapotranspiration that the groundwater body is suffering in successive pumping–irrigation–recharge cycles.

Thus, a deep knowledge of the local hydrogeological conditions and processes controlling salinization is required to understand the feasible actions to take in order to mitigate impacts on water resource systems. In line with this idea, two of the most useful tools to increase the knowledge of complex systems with several variables are multivariate statistical analyses (Hair et al., 1999) and geochemical modeling (e.g., Edmunds, 2009; Zhu and Anderson, 2002). Applications reported in the literature include the use of multivariate analysis to understand the main factor explaining the chemical evolution of waters in regional alluvial aquifers (Acero et al., 2013; Lorite-Herrera et al., 2008). For geochemical modeling, some examples of application are the use of inverse modeling approaches to elucidate the net geochemical reactions occurring in a water flow line from irrigation water to drainage water (Causapé et al., 2004a; García-Garizábal et al., 2014) or the use of direct modeling approaches to reproduce observed patterns in groundwater and to develop simulations in which different hypotheses can be tested (Kim et al., 2005; Stigter et al., 2006). However, both approaches are seldom applied to the same study area, which could improve the knowledge on the processes controlling the hydrological system.

In this context, the objective of the present study is to identify the main geochemical processes related to the salinization of waters in a headwater agricultural basin through the use of both multivariate statistical analysis and geochemical modeling. Specifically, the main aim is to elucidate if the processes controlling salinization of Lerma Basin waters (Merchán et al., 2013, 2014) are related to natural or to anthropogenic factors.

2. Study site description

The Lerma Basin is a small hydrological basin (7.38 km^2, Fig. 1), with 48% of its surface area under irrigation. It is located inside the municipality of Ejea de los Caballeros (Zaragoza, Spain) and is representative, regarding geology, hydrology and agronomy, of a wide range of land–water connected environments in the region (Causapé et al., 2004b).

According to the Spanish National Agency of Meteorology (AEMET, 2014), the climate in the area is Continental to Mediterranean, characterized by extreme temperatures and irregular and scarce precipitations. Temperatures may vary from below zero during winter to as high as 40 °C during summer, with an average temperature of 14 °C. Average annual precipitation during the hydrological years 2004–2011 was around 402 mm and concentrated in spring and autumn (Merchán et al., 2013). Summer and winter are generally dry, only wetted by occasional storms.

The geology in the Lerma Basin is represented by Tertiary and Quaternary materials (Fig. 1). The Tertiary materials appear as a bottom layer (66% of its surface) several hundreds of meters thick, composed of alternating gypsum, clay and silt materials of brown and gray colors, with occasional intercalations of fine limestone layers associated with gypsum (Causapé et al, 2004a; ITGE, 1988). This unit is locally covered by a Quaternary glacis (34% of the surface) up to 10 m thick, dominated by detrital sediments composed of gravels with some Tertiary limestone clasts, alternating with sands, silts and clays (ITGE, 1988). Tertiary materials are exposed due to the erosive effect of a network of gullies developed over the glacis.

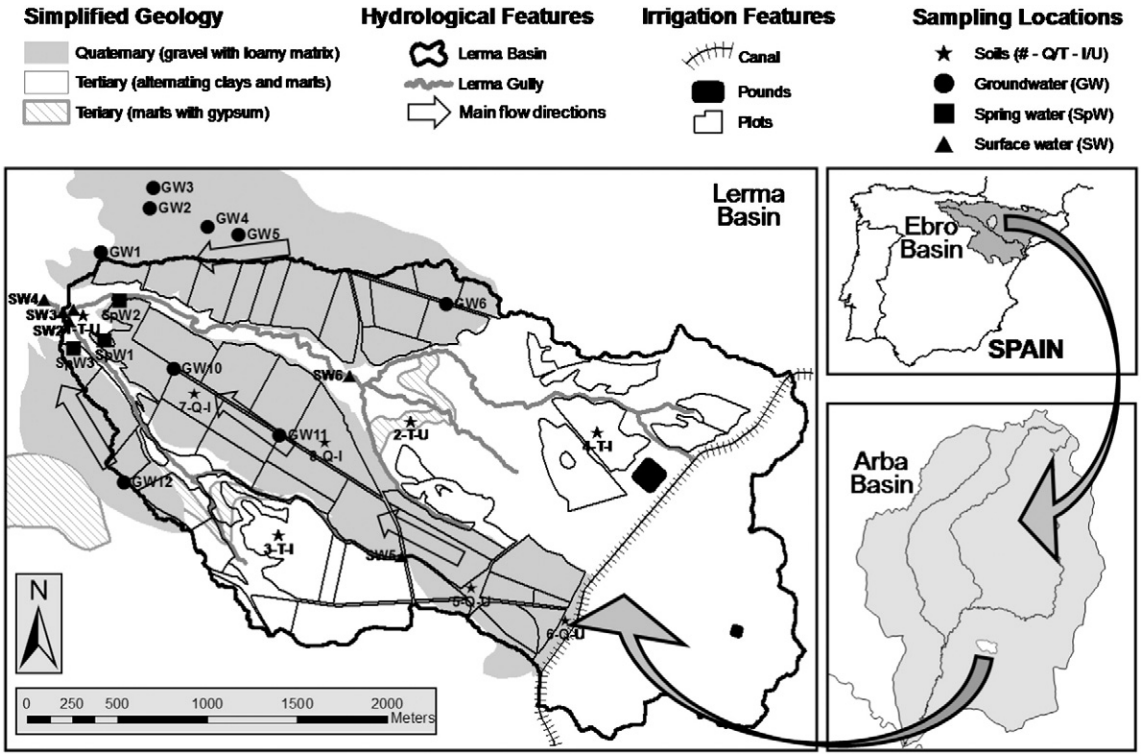

Fig. 1. Location, simplified geology, main hydrological and irrigation features, and sampling locations of the Lerma Basin.

Soils developed on Quaternary glacis (Calcixerollic Xerochrepts, Soil Survey Staff, 2014) display stony loamy textures, 60–90 cm of effective depth, low salinity and small risk of erosion (slope < 3%). On the other hand, soils developed on Tertiary materials (Typic Xerofluvent, Soil Survey Staff, 2014) have 30–45 cm of effective depth, high salinity and significant risk of erosion (slope > 10%). These characteristics identified Quaternary soils as suitable for conversion to irrigated land (Beltrán, 1986) and, in consequence, the irrigated area covers mainly the Quaternary surface (Fig. 1).

Regarding the hydrological behavior, Quaternary materials have medium to high permeability (hydraulic conductivity between 1 and 10 m day^{-1}), constituting free intergranular perched aquifers, whereas Tertiary materials have low permeability. Precipitation and irrigation water infiltrate through Quaternary materials down to the contact with the Tertiary unit, where they flow horizontally over it. Groundwater seeps to the surface through the contact between Quaternary and Tertiary and it feeds a network of gullies. Before irrigation started, these streams flowed mainly during spring and autumn, i.e., the more rainy seasons (Abrahão et al., 2011a) while, after the implementation of irrigation, the Lerma Gully has become a perennial stream.

The Lerma Basin receives water from the Aragón River Basin, via the Bardenas Irrigation Canal, during spring and summer (Fig. 2). Crops cultivated are typical of the Middle Ebro Valley: maize, winter cereal and vegetables. Associated with irrigated agriculture is the application of synthetic fertilizers, mainly through liquid and compound (NPK) fertilizers. It is important to mention the increase in Mg^{2+} in fertilizer applications experienced in recent years in the area, as a consequence of the decrease in this nutrient observed in soils (local fertilization advisors, pers. com.).

3. Methods

3.1. Sampling and chemical analysis of the Lerma Basin waters

Samples of the Lerma Basin waters were collected for chemical analysis in 2011, February the 10th (I) and July the 27th (II), and in 2012, January the 10th (III) and July the 31st (IV) (Fig. 2, Table 2), representing two non-irrigated and two irrigated seasons, along with two low water and two high water seasons, respectively. High waters in the gullies and the Quaternary aquifer took place in the late summer, at the end of the irrigated season. The sampling dates were selected to avoid taking samples in the week after any rainfall event. Sixty-three water samples were collected from the Lerma Basin throughout the study period: groundwaters (GW, 31 samples), spring waters (SpW, 8) and surface waters (SW, 24). These monitoring points were selected after some preliminary analyses were carried out in a broader monitoring scheme. The piezometers were drilled in 2008 in the Quaternary materials to a depth between 6 and 8 m to reach the Tertiary materials and penetrate them around 50 cm further. The Tertiary materials were always dry 20 cm below the contact with the Quaternary materials, which is a proof of their low permeability, since the Quaternary materials just above were saturated. The screened interval covered the whole piezometer.

Groundwater samples were collected using a high density polyethylene bailer, whereas spring or surface water samples were collected manually. In some of the piezometers and sampling campaigns, it was not possible to obtain enough water for analysis since the saturated thickness was lower than the bailer length.

Additionally, all available data of precipitation (P, 11 samples) and irrigation (I, 6 samples) waters, corresponding to samples collected between 2007 and 2012 (Table 2), were included in this study.

Field parameters (electrical conductivity corrected to 25 °C [EC], temperature [T], pH and alkalinity) were measured in situ just after sample collection, with previously calibrated instruments. EC-meter CRISON CM35, and pH-meter CRISON T25 were used for EC, T and pH. Alkalinity was measured using a HACH alkalinity test kit and was similar to that obtained in the laboratory analyses. The filtered samples (0.45 μm) were analyzed within a month of collection. The dissolved ionic concentrations (Na^+, K^+, Ca^{2+}, Mg^{2+}, CO_3^{2-}, HCO_3^-, SO_4^{2-}, Cl^-, NO_3^-) were analyzed by standard analytical methods at the Geological Survey of Spain (IGME) laboratories. Cations were determined by inductively coupled plasma-atomic emission spectrometry (ICP-AES), and anions were analyzed by high performance liquid chromatography (HPLC) technique. The charge balance was cross-checked as follows:

$$Charge\ \ balance\ \ (\%) = 200\frac{\sum meq\ \ cation - \sum meq\ \ anion}{\sum meq\ \ cation + \sum meq\ \ anion}.$$

(Weight, 2008)

Absolute charge balances averaged 2.5% (maximum 6.6%) in precipitation and irrigation waters and 4.4% (maximum 5.8%) in ground, spring and surface waters.

The interpretation of the water quality data was based on the use of indicators of water quality for irrigation purposes (sodium adsorption ratio and Kelly's ratio, related to irrigation water salinity) along with the hydrochemical interpretations (e.g., Piper diagram, ionic ratios).

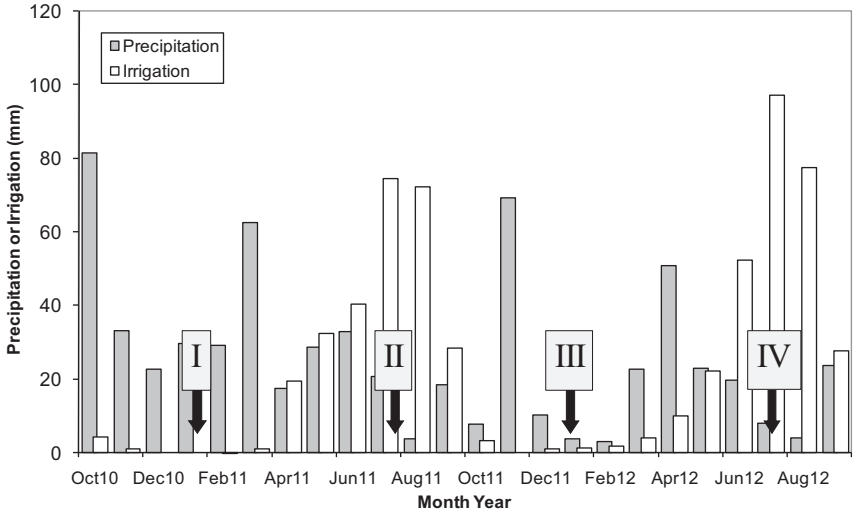

Fig. 2. Precipitation and irrigation in the Lerma Basin during the hydrological years 2010–2012. Sampling campaigns are indicated by black arrows.

The Kruskal–Wallis Test, a non-parametric method for testing whether the samples originate from the same distribution, was used to detect significant differences between groundwater, spring and surface water samples. The statistical package used was Statgraphics Centurion XVI (StatPoint Technologies, 2009).

3.2. Soil leaching experiments

In order to investigate the chemical components that the soils can supply to the waters, a soil sampling campaign was performed in 2013 January 28th. Eight soil samples (stars in Fig. 1) were collected from Tertiary and Quaternary materials in unirrigated and irrigated soils (with two samples in each combination, i.e., Tertiary unirrigated [1 and 2], Tertiary irrigated [3 and 4], Quaternary unirrigated [5 and 6] and Quaternary irrigated soils [7 and 8]), covering all the representative soils and characteristics in the study zone. The samples were collected from the topsoil (up to 25 cm depth). They were treated in the following way: after removing the fraction >2 mm, 100 g of dry sample was mixed with 250 ml of distilled water during 24 h. After this time, the water fraction was extracted, filtered (0.45 μm) and analyzed following the procedure described in the section above. In the preliminary stage, different mixing proportions (250 ml or 500 ml) and mixing times (24, 48 and 96 h) were tested to ensure a complete dilution of the soluble fraction. Results of these preliminary tests were compared through Sign and Signed-Rank Matched Tests (Helsel and Hirsch, 2002) and no significant differences were found what suggests that any of the used amounts of water and experimented contact times were enough to dissolve all the soluble fraction of the materials.

Additionally, mineralogical determinations were performed in the eight soil samples by X-ray diffraction. After removing the fraction >2 mm, around 5 g of dry sample was ground in an agate mortar and pestle and then sieved through 63 μm. X-ray diffraction was performed with XPERT PRO MPD equipment (PANanalytical), and the data were processed using the software HighScore 3.0.4 (PAN analytical). Samples were prepared in the Geochemistry Laboratory of the Earth Sciences Department at the University of Zaragoza, and the X-ray diffraction determinations were performed in the Geological Survey of Spain Laboratories.

3.3. Multivariate statistical analyses

Two multivariate statistical procedures were used to obtain a better understanding of the variety in the data set and the processes involved. The statistical package used was Statgraphics Centurion XVI (StatPoint Technologies, 2009) and the analyses included Principal Components and Hierarchical Cluster. Both were performed on the standardized (Z-scores) hydrochemical data of the 80 water samples from the Lerma Basin (precipitation, irrigation, groundwater, spring and surface waters). The variables included in these analyses were Na^+, K^+, Ca^{2+}, Mg^{2+}; HCO_3^-, SO_4^{2-}, Cl^-, NO_3^- and pH. EC was not included for being a proxy of salinity, represented by the specific cations and anions. The dissolved concentration of CO_3^{2-} was excluded from multivariate analysis since it was below detection limit in most of the samples. For those components occasionally below detection limit, 1/2 of the detection limit value was used.

Principal component analysis (PCA) was performed to infer the controlling variables (components) of the water chemistry. PCA has been widely applied to understand hydrological data (e.g., Morán-Tejeda et al., 2011) and, particularly, hydrogeochemical data: in surface waters (e.g., Cameron, 1996; Evans et al., 1996), groundwater (e.g., Adams et al., 2001; Koh et al., 2007) or both (Lorite-Herrera et al., 2008). PCA summarizes the data set in the minimum components that explain most of the variance. The Varimax method (Davis, 1986) was applied to maximize the variance explained by each component. Each of the new components is a lineal combination of pre-existing standardized variables with different loadings depending on the influence of the variable in that component. For component loadings, an approach similar to that of Evans et al. (1996) or Koh et al. (2007) was selected. A high loading was defined as higher than 0.75, and a moderate loading was defined as between 0.40 and 0.75. Loading of less than 0.40 was considered negligible.

The hierarchical cluster analysis (HCA), commonly applied in hydrological data (e.g., Abrahão et al., 2011b; Causapé et al., 2004a; Menció et al., 2012), was performed here to generate groups of similar samples. Several similarity measurement and linkage methods were tested and the groups obtained were fairly similar. The square Euclidean distance and the Ward method were used to obtain hierarchical associations, since they maximize the homogeneity inside the clusters and maximize heterogeneity between clusters (Hair et al., 1999).

3.4. Geochemical modeling

The USGS software PHREEQC (Parkhurst and Appelo, 1999) with its database *phreeqc.dat* was used for the geochemical modeling as it has been widely applied in all kind of hydrogeochemical problems (e.g., Carol et al., 2009; Edmunds, 2009; Han et al., 2011; van Asten et al., 2003; Zhu and Anderson, 2002). First, speciation-solubility calculations were performed to obtain the saturation indexes (SI) of the different water samples with respect to the mineral phases of interest, particularly, calcite, dolomite, gypsum and halite. Additionally, $CO_2(g)$ partial pressures were also computed based on the alkalinity and pH of the samples (e.g., Kehew, 2001; Appelo and Postma, 2005). Second, an inverse modeling approach, mass balance, was applied between selected water samples considered representative of the variety observed in the data set. Based on the variations in the water chemistry and the observed mineralogy, this approach allowed estimating the net geochemical reactions between samples assumed to be connected by a flow line. Finally, a forward modeling approach was applied using feasible chemical reactions to reproduce the evolution of the system. All the information provided by these geochemical modeling exercises was used to discard or confirm the hypotheses of the different processes inferred throughout the study.

4. Results and discussion

4.1. Soil leaching experiments

Tertiary marly soils (sample 1-T-U) provided the greatest dissolved Na^+ and Cl^- concentrations, 100 and 112 mmol L^{-1}, respectively (Table 1, Fig. 3). Soils over marls with nodular and tabular gypsum (sample 2-T-U) showed the highest dissolved SO_4^{2-}, Ca^{2+} and Mg^{2+} concentrations, 9.6, 4.9 and 8.9 mmol L^{-1}, respectively. The presence of soluble minerals such as halite (NaCl) and gypsum or epsomite ($CaSO_4 \cdot 2H_2O$, $MgSO_4 \cdot 7H_2O$) may explain these results. The samples of Tertiary age that were irrigated (3-T-I and 4-T-I) had values comparable with those of the Quaternary soil samples, probably as a consequence of the different amendments performed by farmers in these irrigated soils (addition of loamy textured soil, plowing, successive wash out of soluble fraction by irrigation water, etc.). Finally, samples from the soils over the Quaternary glacis (5-Q-U, 6-Q-U, 7-Q-I and 8-Q-I) showed the lowest concentrations for the different analyzed ions, with averages of 1.4 mmol L^{-1} for Cl^-, 0.5 mmol L^{-1} for SO_4^{2-}, 0.4 mmol L^{-1} for Na^+, 2.0 mmol L^{-1} for Ca^{2+} and 0.6 mmol L^{-1} for Mg^{2+} (Fig. 3). Thus, the salinity of the waters appears to be mainly controlled by the interaction between the recharge waters (precipitation and irrigation) and the Tertiary substrate.

The X-ray results (Table 1) indicated the predominance of calcite, quartz and clay minerals (mainly illite and chlorite) in all the samples. In fact, these minerals were the only ones detected in the samples from the Quaternary glacis (with the exception of traces of feldspar in some of them). Dolomite, ankerite and gypsum were also identified in the samples taken in the soils over the Tertiary marls and clays

Table 1
Selected soil samples results. Sample: A-B-C where A is the sample ID (1-8), B is a letter presenting the age (T for Tertiary and Q for Quaternary) and C is a letter presenting the land use (I for irrigated and U for unirrigated).

Sample	Description	Stones (wt.% >2 mm)	Water attacks (mmol L^{-1})					X-ray diffractions[a]
			Cl^-	SO_4^{2-}	Na^+	Ca^{2+}	Mg^{2+}	
1-T-U	Marls	0	100.4	3.2	112.3	0.5	1.0	Cal, Qtz, C.M., Dol, Fsp (t)
2-T-U	Marls gyps.	1	50.4	9.6	47.0	4.9	8.9	Cal, Qtz, C.M., Dol/Ank, Gp, Fsp (t)
3-T-I	Marls	2	0.6	1.0	2.1	1.4	0.5	Cal, Qtz, C.M., Dol/Ank, Fsp (t)
4-T-I	Marls	5	0.7	0.4	1.4	1.3	0.6	Cal, Qtz, C.M., Dol/Ank, Fsp (t)
5-Q-U	Glacis	32	0.1	0.1	0.2	1.3	0.5	Cal, Qtz, C.M., Fsp (t)
6-Q-U	Glacis	33	5.0	0.8	0.6	3.3	0.7	Cal, Qtz, C.M.
7-Q-I	Glacis	34	0.3	0.6	0.4	1.5	0.5	Cal, Qtz, C.M., Fsp (t)
8-Q-I	Glacis	45	0.3	0.6	0.5	1.7	0.4	Cal, Qtz, C.M., Fsp (t)

wt.%: percentage in weight.
[a] Cal: calcite; Qtz: quartz; C.M.: clay minerals (illite + chlorite); Dol: dolomite; Fsp: feldspar (t: trace, low intensities); Ank: ankerite; Gp: gypsum.

(Table 1). Despite the useful qualitative information obtained from the X-ray diffraction technique, it was unable to detect soluble mineral phases that could explain Cl^- and Na^+, contents in the waters. However, after a detailed revision of the difractograms, the presence of halite could not be discarded since its signal in diffractograms would overlap with that of other minerals detected. However, epsomite was not detected even after the detailed revision of the diffractograms. Taking the concentrations obtained in sample 1-T-U, the maximum obtained in the soil samples, a fraction of halite of maximum 6% can be estimated from total Na^+ and Cl^- leached and mass of soil used. Consequently, depending on the specific combination of minerals in the sample, it might remain undetected by X-ray diffraction. Similar assumptions can be done with other soluble minerals. In addition, the presence of halite and other soluble minerals is supported by the fact that the Tertiary materials were deposited in a saline lake environment (ITGE, 1988), where the presence of evaporitic minerals is common.

4.2. Hydrogeochemical characterization

Precipitation and irrigation water are the main input waters in the Lerma Basin (Table 2). They have a very low salinity, with typical EC values under 0.05 mS cm^{-1} for precipitation water and under 0.4 mS cm^{-1} for irrigation water. According to their positions in a Piper diagram (Fig. 4), precipitation and irrigation waters are mainly of Ca^{2+}-HCO_3^- type. Both, their low salinity and their water type, indicate a high quality for irrigation purposes, as indicated by several water quality indicators commonly used for irrigation waters. For instance, Sodium Adsorption Rate (SAR) values ranged from 0.04 to 0.55, with an average of 0.23, which indicates a very low sodium hazard in these waters (e.g., Fetter, 2001). Kelly's Ratio (KR) values ranged from 0.07 to 0.58, with an average of 0.19, indicating the good quality of the water for irrigation (Kelly, 1963).

A clear evolution from low salinity Ca^{2+}-HCO_3^- type in the input water to Na^+-mixed-to-Cl^- water type (Fig. 4) with increasing salinity can be observed using the 63 water samples collected in the Lerma Basin (Table 3). Samples with low salinity (an upper stream gully and some piezometers during the irrigation season) belong to the water types closer to precipitation and irrigation waters. There were significant differences (Kruskal–Wallis Test, $p < 0.05$) between the salinity of the groundwaters (average 1.75 mS cm^{-1}) and the salinity of the surface waters (average 2.63 mS cm^{-1}) while spring waters had intermediate salinity values. Thus, the quality of water for irrigation purposes decreases between recharge waters and water in the outlet of the basin, presenting slight restriction for irrigation purposes (EC > 0.7 mS cm^{-1}, Ayers and Westcost, 1992). In fact, some surface waters and the groundwater point GW12 in 2012 presented severe restriction for irrigation purposes (EC > 3 mS cm^{-1}). This decrease in quality is also indicated by the SAR values from 0.45 to 10.77, with a medium value of 5.76 (low to medium sodium hazards, e.g., Fetter, 2001) and KR values from 0.15 to 2.47, with an average value of 1.34 (waters with values higher than one are considered unsuitable for irrigation purposes, Kelly, 1963).

Additionally, significant differences (Kruskal–Wallis Test, $p < 0.05$) were observed in the physicochemical parameters and the major ions median content between ground and surface waters (Table 3). Significantly higher values in pH, Cl^-, SO_4^{2-}, Na^+, Ca^{2+}, and Mg^{2+}, and lower values in NO_3^- were observed in surface waters compared with groundwater. Spring waters showed values generally closer to those of groundwater except in the case of pH that they are

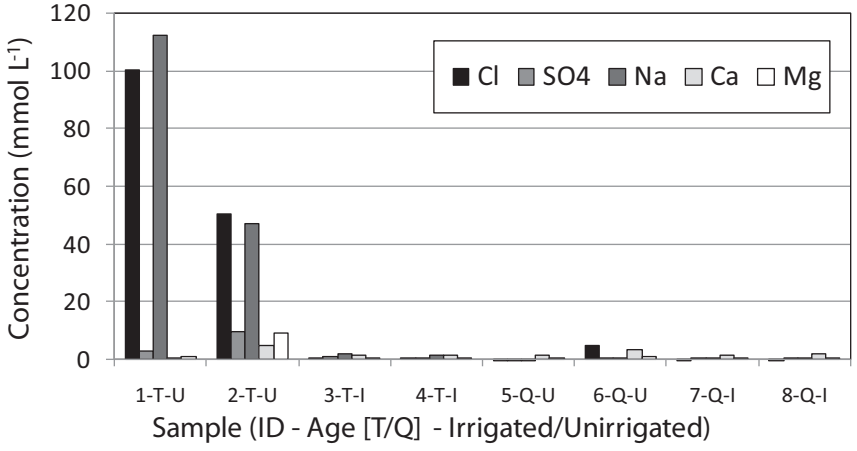

Fig. 3. Concentration of major ions after 24 h of contact and mixing between soil samples (100 g) and distilled water (250 g). Sample codification: A-B-C where A is the sample ID (1–8), B is a letter presenting the age of the materials (T for Tertiary and Q for Quaternary) and C is a letter presenting the land use (I for irrigated and U for unirrigated).

Table 2
Precipitation and irrigation hydrochemical data available from the Lerma Basin.

Sample	Date	EC mS cm^{-1}	pH	Ca^{2+}	Mg^{2+}	Na^{+}	K^{+}	CO_3^{2-}	HCO_3^{-}	SO_4^{2-}	Cl^{-}	NO_3^{-}	C.B. %
				mmol L^{-1}									
P	16/11/2009	0.053	7.08	0.10	0.25	0.20	0.05	b.d.l.	0.38	0.06	0.14	0.00	4.0
P	15/12/2009	0.041	6.32	0.10	0.25	0.07	0.03	b.d.l.	0.29	0.05	0.06	0.03	2.3
P	19/01/2010	0.015	5.38	0.05	0.08	0.04	0.01	b.d.l.	0.11	0.03	0.03	0.01	−2.8
P	15/03/2010	0.048	5.58	0.45	0.08	0.04	0.00	b.d.l.	0.41	0.04	0.03	0.08	3.2
P	13/05/2010	0.045	5.43	0.40	0.08	0.06	0.01	b.d.l.	0.29	0.10	0.04	0.10	3.3
P	21/11/2011	0.008	5.03	0.10	b.d.l.	0.01	b.d.l.	b.d.l.	0.07	0.03	0.01	0.01	−6.6
P	17/11/2011	0.007	4.86	0.10	b.d.l.	0.02	b.d.l.	b.d.l.	0.07	0.03	0.02	0.01	−1.5
P	03/05/2012	0.029	6.56	0.10	0.16	0.03	b.d.l.	b.d.l.	0.21	0.03	0.02	0.03	−0.3
P	23/05/2012	0.032	5.15	0.05	0.25	0.10	0.01	b.d.l.	0.20	0.05	0.13	0.02	1.9
P	22/10/2012	0.027	7.50	0.10	0.16	0.02	b.d.l.	b.d.l.	0.25	0.01	0.01	0.00	5.3
P	08/11/2012	0.015	6.39	0.05	0.08	0.01	b.d.l.	b.d.l.	0.11	0.01	0.01	0.01	3.1
Average		0.039	5.71	0.15	0.13	0.05	0.01	–	0.22	0.04	0.05	0.03	
SD		0.017	0.76	0.14	0.09	0.06	0.02	–	0.12	0.02	0.05	0.03	
I	22/10/2007	0.360	n.a.	2.40	0.72	0.63	0.03	b.d.l.	2.56	0.55	0.66	n.a.	0.1
I	12/11/2007	0.380	n.a.	2.48	0.72	0.64	0.03	b.d.l.	2.64	0.48	0.78	n.a.	−0.9
I	24/07/2008	0.330	n.a.	2.87	0.48	0.27	0.02	b.d.l.	3.05	0.29	0.30	n.a.	0.0
I	17/09/2008	0.280	n.a.	2.40	0.64	0.30	0.03	b.d.l.	2.62	0.34	0.40	n.a.	0.1
I	27/07/2011	0.318	8.10	1.95	0.74	0.64	0.03	0.08	2.38	0.35	0.44	0.02	3.0
I	31/07/2012	0.318	8.10	2.30	0.16	0.43	0.01	b.d.l.	2.38	0.29	0.32	0.02	−3.5
Average		0.334		2.40	0.58	0.49	0.02	–	2.60	0.38	0.48	–	
SD		0.039		0.30	0.22	0.18	0.01	–	0.25	0.11	0.19	–	

SD: standard deviation. n.a.: not available. b.d.l.: below detection limit. C.B.: charge balance.

closer to those of surface waters. No significant differences were detected for HCO_3^{-} and K^{+} values.

4.3. Ionic ratios

Ionic ratios in hydrochemical data have been useful in providing an insight into the hydrogeochemical processes controlling the changes in water quality. The molar ratio Na^{+}/Cl^{-} ranged from 0.75 to 4.91 (Fig. 5A), with low values for precipitation and irrigation waters (0.75–1.62) and also for surface waters (1.07–1.76), slightly higher values for springs (1.36–2.31) and the highest values in some groundwaters (0.90–4.91). A trend towards values close to 1.00 was observed with increasing salinity, which can be attributed to halite dissolution although in the samples with the lowest salinity an additional source of sodium is required. Ionic exchange could provide sodium to these low salinity samples (e.g., Lorite-Herrera et al., 2008), especially considering that irrigation water with low salinity and significant Ca^{2+} concentrations is added to soils, which favors the ionic exchange in this direction (Na^{+} enters the solution, Ca^{2+} leaves the water solution, Appelo and Postma, 2005).

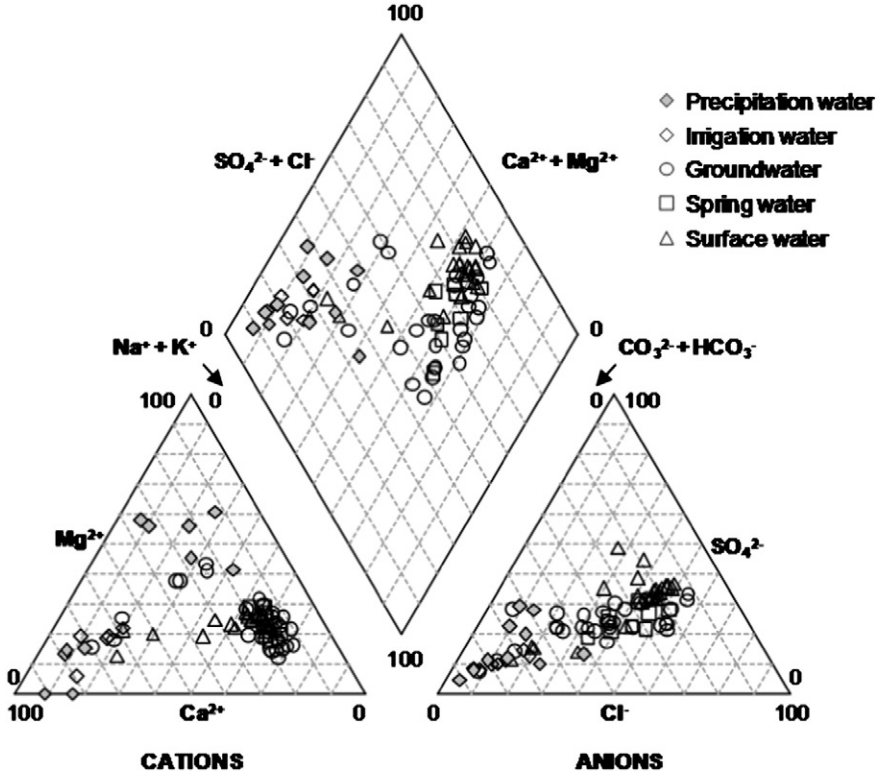

Fig. 4. Piper diagram showing the situation of the Lerma Basin waters.

Table 3
Surface (gullies, G), spring (S) and groundwater (wells, W) hydrochemical data available from the Lerma Basin.

Date		EC mS cm^{-1}	pH	T °C	Ca^{2+}	Mg^{2+}	Na^{+}	K^{+}	CO_3^{2-}	HCO_3^{-}	SO_4^{2-}	Cl^{-}	NO_3^{-}	C.B. %
					mmol L^{-1}									
GW1-I	10-02-2011	1.43	7.9	10.1	2.59	2.88	10.20	0.21	b.d.l.	5.74	3.21	3.62	2.45	5.6
GW3-I	10-02-2011	1.48	7.8	10.8	3.04	3.37	14.42	0.08	b.d.l.	5.90	3.90	8.06	2.13	4.5
GW4-I	10-02-2011	1.39	8.0	13.0	1.95	2.30	10.48	0.09	b.d.l.	4.36	3.09	3.79	2.82	5.3
GW5-I	10-02-2011	1.67	7.8	13.4	3.39	3.87	11.49	0.15	b.d.l.	5.90	2.43	5.53	4.08	5.0
GW10-I	10-02-2011	1.63	7.8	11.6	2.79	5.76	10.48	0.21	b.d.l.	6.29	3.77	5.85	2.32	5.4
GW11-I	10-02-2011	1.52	7.6	13.4	4.04	7.49	5.53	0.17	b.d.l.	6.23	3.63	5.94	1.85	−2.4
GW12-I	10-02-2011	2.53	7.7	11.9	3.49	6.34	17.99	0.09	b.d.l.	6.39	7.62	10.92	1.54	5.3
SW1-I	10-02-2011	2.49	8.4	6.5	5.14	5.92	17.25	0.19	b.d.l.	6.88	8.41	10.70	1.20	4.7
SW2-I	10-02-2011	4.25	8.4	6.1	9.58	12.51	23.74	0.15	b.d.l.	6.72	15.29	21.52	1.18	2.8
SW3-I	10-02-2011	3.14	8.4	6.1	5.84	9.13	19.45	0.14	b.d.l.	7.05	10.30	14.10	1.23	5.6
SW4-I	10-02-2011	3.17	8.5	6.2	5.64	9.13	19.78	0.15	b.d.l.	7.18	10.31	14.19	1.22	5.3
SW5-I	10-02-2011	0.46	8.5	5.7	2.50	0.99	1.39	0.04	b.d.l.	3.02	0.72	0.93	0.03	4.8
SW6-I	10-02-2011	2.66	8.5	5.2	6.39	7.74	15.92	0.14	b.d.l.	6.72	10.88	10.85	0.13	5.4
GW1-II	27-07-2011	1.32	7.6	19.0	3.19	2.63	11.90	0.18	0.12	7.93	2.99	3.81	2.19	5.0
GW4-II	27-07-2011	1.31	7.6	16.8	2.45	2.63	10.14	0.11	0.16	5.70	2.59	3.56	2.66	4.3
GW5-II	27-07-2011	0.49	7.4	16.9	3.44	0.74	0.65	0.10	0.16	3.18	0.43	0.50	0.56	−0.4
GW6-II	27-07-2011	1.40	7.9	21.6	3.44	4.85	9.16	0.06	0.04	8.06	4.06	3.30	1.15	5.3
GW10-II	27-07-2011	1.64	7.5	17.6	2.99	6.09	10.44	0.22	0.20	7.31	3.38	5.73	2.27	4.4
GW11-II	27-07-2011	1.15	7.4	16.4	3.24	5.27	4.33	0.14	0.16	7.08	3.09	0.88	1.28	3.9
GW12-II	27-07-2011	2.79	7.5	17.7	4.24	6.91	18.26	0.10	0.08	5.11	7.38	14.17	1.61	4.0
SpW1-II	27-07-2011	1.81	7.5	21.1	2.94	4.11	13.36	0.13	0.12	8.29	3.26	5.77	2.10	5.0
SpW2-II	27-07-2011	1.78	8.2	18.9	3.19	5.60	12.12	0.20	0.08	6.56	4.29	6.33	2.73	5.5
SpW3-II	27-07-2011	2.63	8.2	21.4	5.14	5.18	18.53	0.07	b.d.l.	7.08	4.97	11.34	3.90	5.8
SW1-II	27-07-2011	2.60	8.2	18.8	4.64	6.50	17.30	0.17	b.d.l.	6.88	7.94	11.15	1.25	5.0
SW2-II	27-07-2011	4.28	8.2	16.5	7.69	10.86	32.78	0.14	b.d.l.	9.67	16.54	21.56	0.92	5.5
SW3-II	27-07-2011	3.30	8.3	17.4	6.14	8.89	20.74	0.16	b.d.l.	6.69	11.44	15.62	1.12	3.0
SW4-II	27-07-2011	3.32	8.2	16.5	5.99	9.13	20.16	0.16	b.d.l.	6.88	11.37	15.72	1.12	1.0
SW5-II	27-07-2011	0.36	8.3	22.6	2.30	0.82	0.78	0.03	0.08	2.72	0.42	0.57	0.01	3.2
SW6-II	27-07-2011	1.83	8.2	20.7	5.74	5.02	10.70	0.17	b.d.l.	7.08	7.15	6.10	0.09	5.7
GW1-III	10-01-2012	1.60	7.9	10.5	2.74	1.81	10.15	0.21	b.d.l.	3.82	3.30	4.04	2.95	5.6
GW3-III	10-01-2012	2.11	7.7	10.8	3.29	2.96	13.96	0.12	b.d.l.	4.51	3.90	9.08	1.77	5.4
GW4-III	10-01-2012	1.45	7.8	14.0	2.50	1.81	8.57	0.08	b.d.l.	3.05	2.64	3.79	2.76	5.7
GW5-III	10-01-2012	1.49	7.7	13.8	3.44	2.80	8.28	0.11	b.d.l.	3.82	2.43	3.84	3.74	5.6
GW6-III	10-01-2012	2.86	7.9	9.0	3.94	8.72	16.39	0.10	b.d.l.	6.29	8.06	11.41	1.90	5.2
GW10-III	10-01-2012	2.22	7.8	12.4	2.64	5.84	14.87	0.16	b.d.l.	4.74	4.68	10.72	2.18	5.2
GW11-III	10-01-2012	2.27	7.6	13.7	3.69	5.76	12.64	0.13	b.d.l.	5.08	5.69	8.29	1.97	5.5
GW12-III	10-01-2012	3.03	8.0	13.4	3.94	7.24	18.82	0.09	b.d.l.	3.46	8.32	14.73	2.00	5.4
SpW2-III	10-01-2012	2.04	8.4	9.5	3.19	5.02	11.48	0.17	b.d.l.	4.62	5.20	7.21	2.06	5.8
SpW3-III	10-01-2012	2.84	8.4	6.8	4.94	4.61	17.54	0.07	b.d.l.	4.31	6.19	11.51	3.74	5.3
SW1-III	10-01-2012	2.96	8.2	3.8	4.04	5.60	15.45	0.11	b.d.l.	4.75	7.82	9.92	1.36	5.5
SW2-III	10-01-2012	3.33	8.3	2.9	5.54	7.90	17.40	0.09	b.d.l.	4.03	10.46	13.99	0.87	5.2
SW3-III	10-01-2012	2.95	8.3	2.8	4.79	6.25	16.56	0.10	b.d.l.	4.54	8.87	11.63	1.17	5.6
SW4-III	10-01-2012	2.97	8.3	2.2	4.74	6.50	16.72	0.10	b.d.l.	4.39	9.06	11.93	1.15	5.6
SW5-III	10-01-2012	0.40	8.4	3.7	2.10	0.41	0.72	0.03	b.d.l.	2.03	0.50	0.58	0.02	4.0
SW6-III	10-01-2012	2.08	8.3	2.5	4.99	4.20	9.81	0.10	b.d.l.	3.39	8.01	6.65	0.05	5.3
GW1-IV	31-07-2012	1.70	7.5	18.6	3.49	2.47	10.89	0.21	b.d.l.	6.42	3.07	4.40	2.98	0.3
GW2-IV	31-07-2012	1.17	7.8	19.6	2.45	2.22	7.43	0.13	b.d.l.	5.57	2.24	2.40	1.63	3.2
GW3-IV	31-07-2012	1.35	7.5	18.9	4.39	1.97	1.38	0.03	b.d.l.	6.36	0.55	0.65	0.28	−0.8
GW4-IV	31-07-2012	0.90	7.6	18.7	3.04	3.21	2.32	0.08	b.d.l.	4.10	1.64	1.67	1.36	−1.2
GW5-IV	31-07-2012	0.49	7.9	18.5	2.55	0.74	0.74	0.07	b.d.l.	2.67	0.52	0.58	0.45	−3.8
GW6-IV	31-07-2012	1.64	7.5	20.0	5.84	6.42	4.92	0.09	b.d.l.	5.77	3.10	5.44	2.65	1.6
GW10-IV	31-07-2012	2.42	7.6	18.1	2.94	5.60	18.05	0.18	b.d.l.	5.47	5.00	12.87	2.01	5.4
GW11-IV	31-07-2012	2.42	7.5	17.3	3.29	6.67	15.08	0.12	b.d.l.	5.01	5.20	12.07	1.54	5.5
GW12-IV	31-07-2012	3.25	7.8	23.5	4.59	8.56	20.67	0.11	b.d.l.	4.02	10.99	17.80	1.44	0.9
SpW1-IV	31-07-2012	1.80	7.9	27.3	3.64	5.43	9.81	0.21	b.d.l.	5.44	3.69	7.10	1.84	5.5
SpW2-IV	31-07-2012	2.20	8.2	23.1	3.44	6.75	13.35	0.18	b.d.l.	5.38	5.50	9.80	1.91	4.9
SpW3-IV	31-07-2012	2.58	8.0	23.3	5.14	5.35	17.22	0.07	b.d.l.	9.18	4.78	9.15	3.18	5.5
SW1-IV	31-07-2012	2.25	8.2	18.6	4.44	5.27	13.99	0.17	b.d.l.	6.82	4.35	8.31	3.07	5.7
SW2-IV	31-07-2012	4.23	8.2	16.7	9.28	12.01	23.51	0.13	b.d.l.	7.57	16.47	22.00	0.86	-4.3
SW3-IV	31-07-2012	3.31	8.1	17.2	7.09	8.64	19.14	0.16	b.d.l.	7.01	10.30	15.08	1.94	2.0
SW4-IV	31-07-2012	3.36	8.2	17.5	7.29	8.64	19.34	0.15	b.d.l.	7.11	10.40	15.02	1.89	2.8
SW5-IV	31-07-2012	1.03	8.1	22.6	3.84	1.97	4.58	0.06	0.12	5.38	1.44	3.37	0.16	−0.2
SW6-IV	31-07-2012	2.48	7.9	20.0	8.98	7.24	13.01	0.12	b.d.l.	6.52	13.28	7.38	0.54	5.7

b.d.l.: below detection limit. C.B.: charge balance.

The Cl^{-} vs. SO_4^{2-} plot (Fig. 5B) shows the strong correlation between both solutes, suggesting an origin from the same source, i.e., high salinity Tertiary materials, as inferred in the soil leaching experiments. The molar ratio Ca^{2+}/SO_4^{2-} (Fig. 5C) ranged from 8.0 to 0.4, showing a clear decrease with salinity. Since average values in precipitation and irrigation water were around 4.9 either supplementary sulfate sources apart from gypsum or Ca^{2+} sinks (or both) are required to explain such a decrease. A similar pattern was observed for the ratio $(Ca^{2+} + Mg^{2+})/SO_4^{2-}$ (not shown), which also decreases with increasing salinity towards a value of 1.0. In fact, the plot SO_4^{2-} vs. $(Ca^{2+} + Mg^{2+})$ (Fig. 5D) presented a strong correlation coefficient ($R^2 = 0.89$) with a better fit equation of $(Ca^{2+} + Mg^{2+}) = 1.14 \cdot SO_4^{2-} + 2.51$. This indicates that similar amounts (in molar ratios) of $Ca^{2+} + Mg^{2+}$ and SO_4^{2-} (slope of

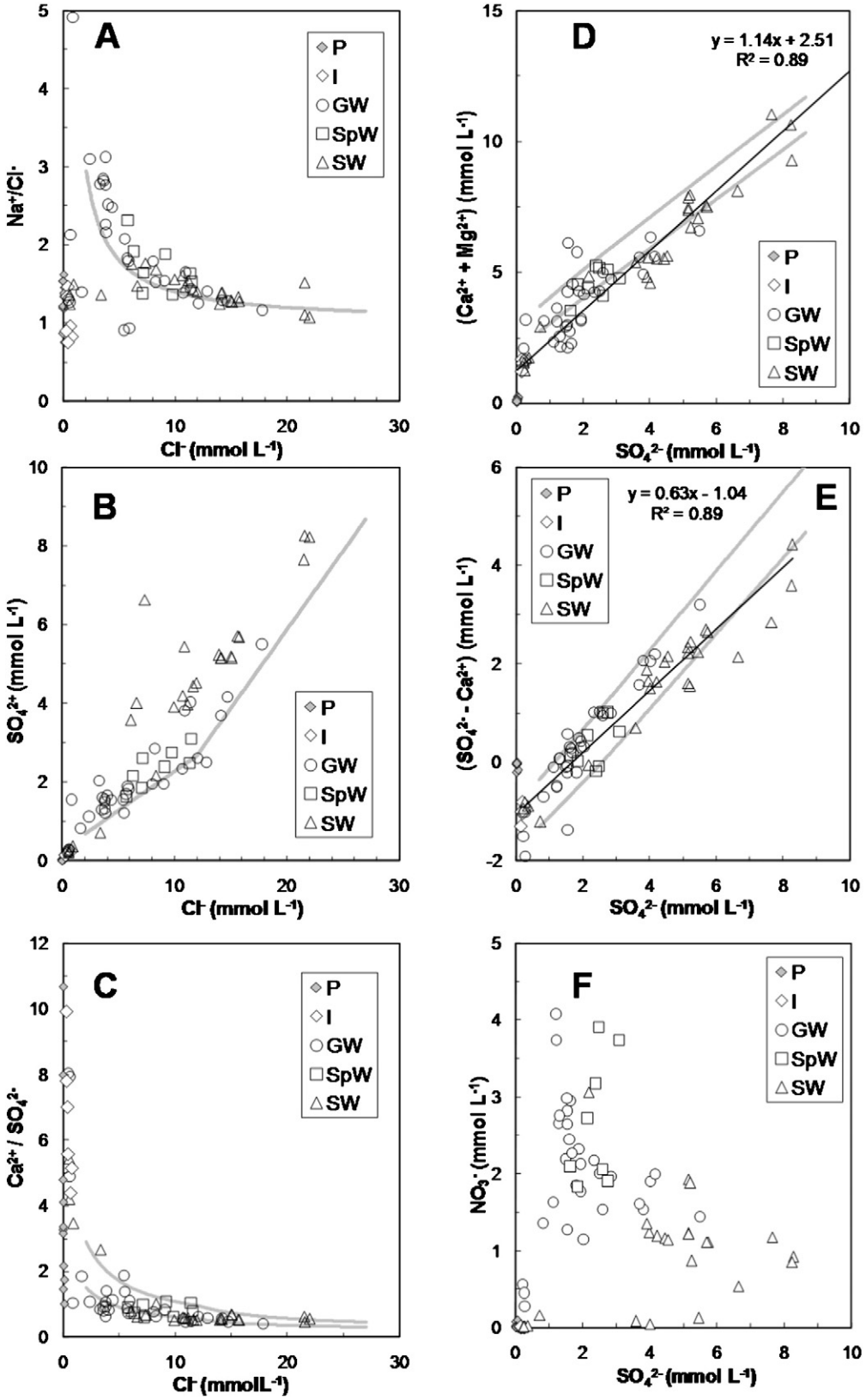

Fig. 5. Ionic ratio evolution with the increase in salinity, indicated by both chloride and sulfate. The gray line represents the geochemical evolution simulated with PHREEQC. Legend: P: precipitation; I: Irrigation; GW: groundwater; SpW: spring water; SW: surface water. When two lines are presented, they cover a range of partial pressures of CO_2 (from $10^{-2.5}$ to 10^{-3}) used in the simulations.

1.14) are being added to the water. The value for zero sulfate (intercept of 2.51) responds to the high Ca^{2+} low SO_4^{2-} irrigation or precipitation water.

The molar ratio $(Ca^{2+} + Mg^{2+})/HCO_3^-$ (not shown) ranged from 0.7 to 3.3, and it increased with salinity, which indicates a supplementary source of $Ca^{2+} + Mg^{2+}$ with respect to HCO_3^-, probably the dissolution

of non-carbonate minerals rich in Ca^{2+} and Mg^{2+} (e.g., gypsum, epsomite). The enrichment in these components may also be related to the addition of mineral fertilizers, as Ca^{2+} and Mg^{2+} are reported to suffer significant increases in areas under extensive application of synthetic fertilizers (Moussa et al., 2011; Stigter et al., 2006).

The plot $(Ca^{2+} + Mg^{2+} - SO_4^{2-} - HCO_3^-)$ vs. $(Na^+ + K^+ - Cl^-)$ (not shown) examines the excess of Ca^{2+} and Mg^{2+} gained or lost from gypsum, calcite and dolomite dissolution/precipitation, and the excess of Na^+ and K^+ gained or lost from sodium and potassium chlorides dissolution/precipitation, respectively. When dissolution of these minerals is enough to explain the hydrochemical composition, the samples plot around the origin. In the Lerma Basin waters, the samples presented a distribution so that a decrease in $(Ca^{2+} + Mg^{2+} - SO_4^{2-} - HCO_3^-)$ was observed with increases in $(Na^+ + K^+ - Cl^-)$, what suggests the existence of important cationic exchange or silicate weathering processes (Jalali, 2005, 2007).

The plot SO_4^{2-} vs. $(SO_4^{2-} - Ca^{2+})$ (Fig. 5E) displays the amount of SO_4^{2-} exceeding Ca^{2+} contents. Assuming that all the SO_4^{2-} has its origin in gypsum dissolution, this plot represents the amount of Ca^{2+} removed by either ionic exchange or calcite precipitation. In waters with very low salinity, the negative values belong to the high Ca^{2+} low SO_4^{2-} Ca^{2+}-HCO_3^- irrigation water type. A slope of ca. 0.6 with increasing salinity suggests that around half of the Ca^{2+} incorporated in gypsum dissolution may be lost through exchange reactions, calcite precipitation or both.

The evolution of previous ratios could be explained by the dissolution of gypsum in waters previously saturated with respect to calcite, with the consequent incongruent dissolution of dolomite (Kehew, 2001). The addition of Ca^{2+} will produce the precipitation of calcite (removing part of the Ca^{2+} added) and the concomitant dissolution of dolomite (adding Mg^{2+} to the water). Another explanation can be related to the hypothetical presence of Mg^{2+}-bearing mineral (e.g., epsomite) or the addition of Mg^{2+} through fertilization.

Finally, the plot SO_4^{2-} vs. NO_3^- (Fig. 5F) showed a lack of relationship between these two solutes, which may suggest different sources for them (Li et al., 2006). Many earlier studies have related high SO_4^{2-} levels to agricultural activities (e.g., Moussa et al., 2011; Kim et al., 2005; Sánchez et al., 2007) by means of its relationship to nitrate pollution, although there are cases in which this pattern is not present. However, the amount of sulfate originated in agricultural activities in the Lerma Basin waters seems to be negligible in comparison with that provided by the geological materials in the study area.

Thus, through the use of the ionic ratios the main processes controlling the evolution of the Lerma Basin water have been inferred. Cation exchange processes are probable, especially in the first phases of the geochemical evolution, i.e., the percolation through soils and the early stages of circulation in the Quaternary aquifers. After this, a pattern controlled by the dissolution of both halite and gypsum may explain the later phases in the geochemical evolution. Dissolution of gypsum probably triggers calcite precipitation and the concomitant dolomite dissolution, although dolomite dissolution kinetics is slow in comparison with the remaining processes and other magnesium sources can participate. The information generated in this section will be used later (saturation indexes and geochemical modeling) to test if these processes are thermodynamically feasible.

4.4. Speciation-solubility calculations

Speciation-solubility calculations provided the saturation indexes (SI) of several mineral phases (calcite, dolomite, gypsum and halite) and the CO_2(g) partial pressure in the different water samples of the Lerma Basin (Fig. 6).

Precipitation waters were highly undersaturated (SI < 0) with respect to all the considered mineral phases. However, irrigation waters were oversaturated (SI > 0) with respect to calcite and dolomite (Fig. 6A and 6B) whereas they were undersaturated (SI < 0) with respect to gypsum and halite (Fig. 6C and 6D). Irrigation waters came from a surface water reservoir in the Pyrenean Range with many carbonate aquifers in its recharge area. The conveyance of these waters in surface canals favors its degasification, which explains the oversaturation of these waters with respect to the carbonate minerals.

Significant differences were observed between ground- and surface waters. Most of them were in equilibrium or oversaturated with respect to calcite and dolomite (Fig. 6A and 6B), although SI values were slightly higher for surface waters (e.g., calcite $SI_{average}$ is 0.27 for groundwater and 0.93 for surface water). The same happens with respect to gypsum and halite, although both, ground- and surface waters, are undersaturated (SI < 0) the SI values were higher for surface waters (e.g., gypsum $SI_{average}$ is −1.6 for groundwater and −1.2 for surface waters; Fig. 6C and 6D). Calcite and dolomite SI were independent of EC, whereas gypsum and halite SI tend to increase with EC, pointing to the dissolution of these minerals as one of the reasons for the increase of salinity. In both cases, spring waters had an intermediate value between ground- and surface waters.

The partial pressure of CO_2(g) (pCO_2) shows significant differences between ground- ($pCO_{2\text{-average}} = 10^{-2.3}$), spring ($pCO_{2\text{-average}} = 10^{-2.6}$) and surface waters ($pCO_{2\text{-average}} = 10^{-2.9}$) (Fig. 6E). As expected, the values were higher in the groundwaters due to the presence of organic matter in soils, roots respiration and microbial decomposition (Kehew, 2001). A pattern of lower CO_2 with higher SI for calcite was inferred (Fig. 6F) suggesting degasification of the water in the flow from ground- to surface waters. Surface waters show values closer to equilibrium with atmospheric CO_2 but still higher than those of the atmospheric partial pressure, indicating that these waters will still lose CO_2 and, probably, precipitate calcite.

In summary, the results obtained for the saturation indexes and the pCO_2 supported the geochemical processes inferred previously, especially regarding gypsum and halite dissolution and calcite precipitation, which are thermodynamically favored.

4.5. Multivariate statistical analysis

4.5.1. Principal component analysis (PCA)

PCA results indicated that two components explained most of the variance (82%, Fig. 7). Component 1 had high loadings for SO_4^{2-}, Cl^-, Mg^{2+}, Ca^{2+} and Na^+, while it had moderate loadings for HCO_3^- and pH. It had insignificant loadings for NO_3^- and K^+. Component 1 can be interpreted as indicating the salinization occurring in the Lerma Basin waters, mainly through the dissolution of minerals bearing the above mentioned components. This component explained 68.8% of the dataset variance.

Component 2 appeared to be related to nitrate contamination as the NO_3^- loading was clearly higher than any other (Fig. 7). Also high loadings were detected for K^+, which can be related to the join application of nitrogen and potassium fertilizers (NPK, Otero et al., 2005). In addition, Component 2 presented moderate loadings of HCO_3^-, pH and Na^+. This factor explained 13.2% of the dataset variance. Those variables that presented high loadings for Component 2 presented low values for Component 1, and vice versa. This suggested independence in the processes controlling the geochemical evolution.

Thus, the main conclusion obtained after the PCA application was the isolation of the processes regarding the main problems in the study area, i.e., the salinization and nitrate pollution processes. Whereas the salinization process explained most of the variability in the dataset, it was not related to nitrate pollution and, as a consequence, to fertilizers applied in agriculture. Thus, nitrate pollution does not seem to affect the contents of dissolved solids in this study zone. These results contrast with those of Nakano et al. (2008) or Moussa et al. (2011), among others, who reported a relationship between salinization and nitrate pollution processes in agricultural areas in Japan and Tunisia, respectively. However, Lorite-Herrera et al. (2008) reported a case for the hydrogeochemistry of a regional alluvial aquifer in the Guadalquivir

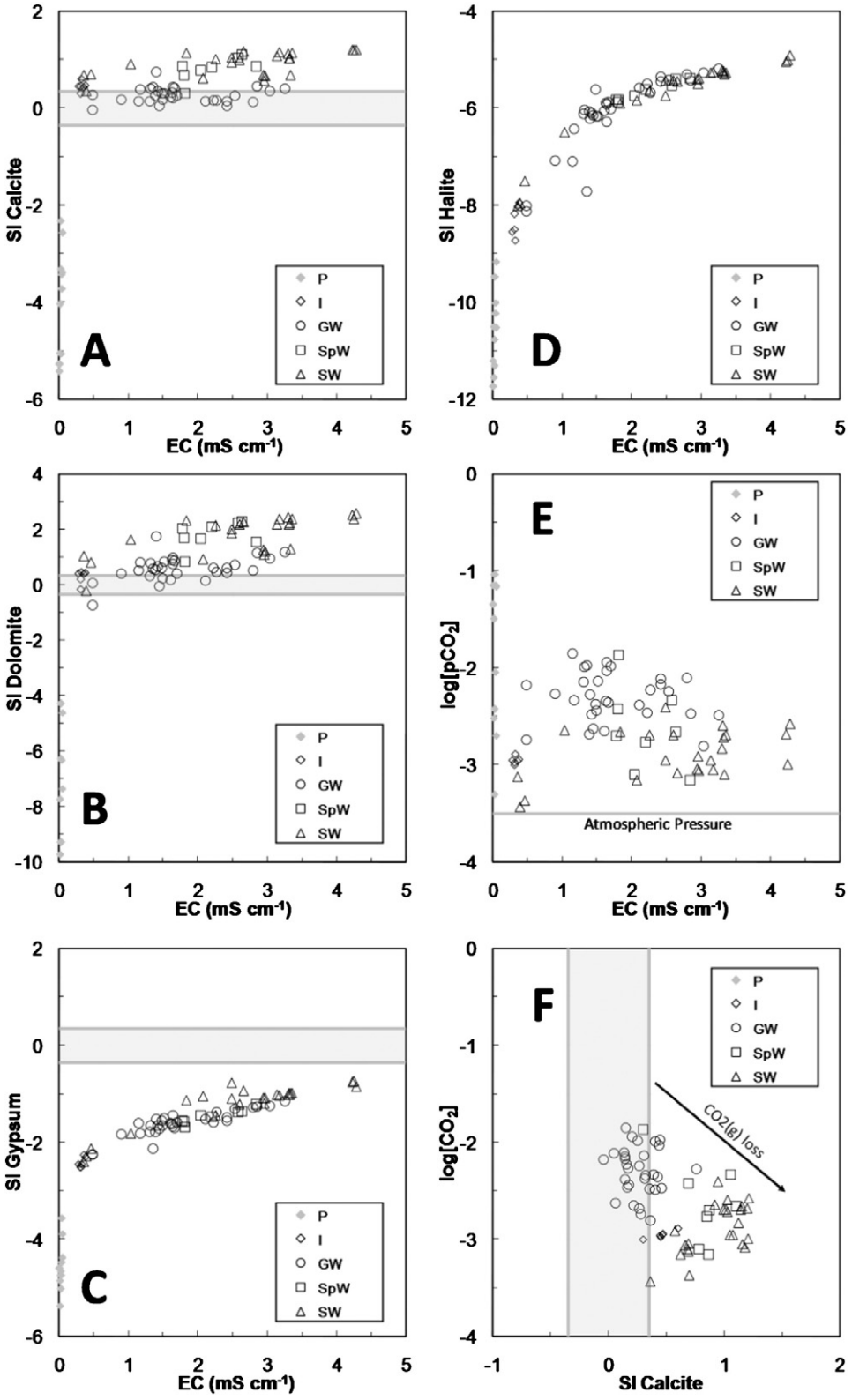

Fig. 6. Evolution with salinity (indicated as electrical conductivity) of saturation indexes of calcite (A), dolomite (B), gypsum (C), halite (D) and partial pressure of CO_2 (E). Partial pressure of CO_2 against calcite saturation index (F). Legend: P: precipitation; I: irrigation; GW: groundwater; SpW: spring water; SW: surface water. The shaded areas indicate the ranges of uncertainty for the calculated saturation indexes; ±0.22 for gypsum (Langmuir and Melchior, 1985), ±0.35 for calcite and ±0.5 for dolomite (Plummer et al., 1990).

River Basin (Spain) where salinization processes were not related to nitrate pollution. Thus, the relationship between salinization and nitrate pollution seems to depend on the specific characteristics of the study zone, with the expected influence of the natural salinity of the area. Apparently, the higher the natural salinity, the lower the influence of agriculture in the salinization of water bodies. However, the

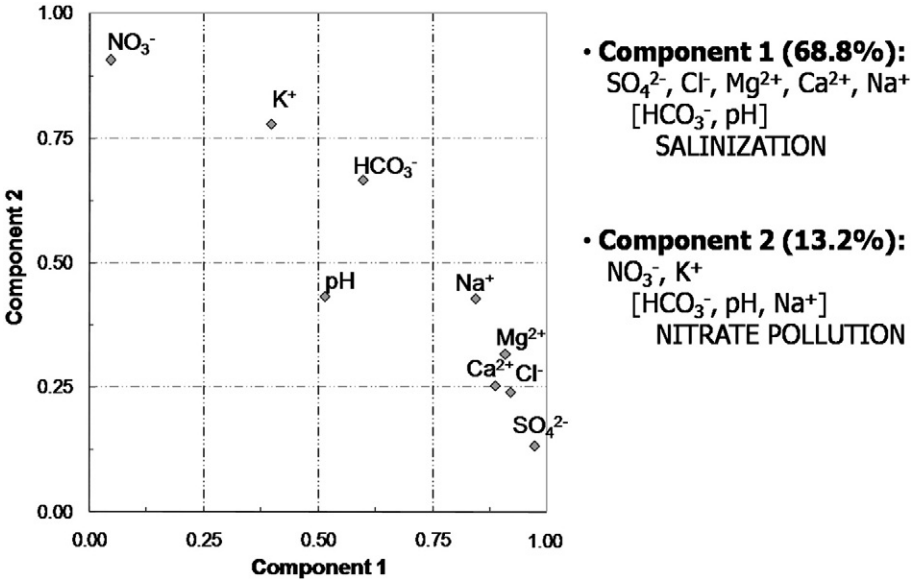

Fig. 7. Component loading diagrams for variables obtained after principal component analysis for Component 1 and Component 2. Variance of dataset explained, variables with high loading and moderate loading (in brackets) and main related process.

influence of salts provided by agriculture should be considered in low-salinity water bodies.

4.5.2. Hierarchical cluster analysis (HCA)

HCA results allowed the association of the Lerma Basin samples in two different branches (Fig. 8). Branch 1 grouped the recharge waters, and was divided into two sub-branches. Branch 1.1 included all the samples of the precipitation water (P) whereas Branch 1.2 included all the samples of irrigation water (I) along with several samples of groundwater and a sampling point of surface water. These ground- and surface water samples were highly influenced by the recharge water. The SW5 sampling point is located in an area dominated by low salinity Quaternary materials and it is close to the irrigation canal, probably receiving some seepage from it (Fig. 1). Samples in branch 1.2 of wells GW3, GW4 and GW5 correspond to the irrigated season, when the aquifer is highly influenced by the recharge of irrigation water (Fig. 8).

Branch 2 grouped most of the collected samples (69%) and it had two different subgroups. Branch 2.1 included most of the groundwater samples collected and all the spring samples, which was coherent since non-significant differences were detected between these two groups and non-significant changes in the water chemistry were found in the groundwater flow lines. Branch 2.2 included most of the surface water samples, which had a higher salinity in general, along with several groundwater samples (locations GW12 and GW6). These wells were located in the vicinity of the more gypsum-rich layer in the basin, which can explain its enrichment in salts and its similarity to the surface water (Fig. 1).

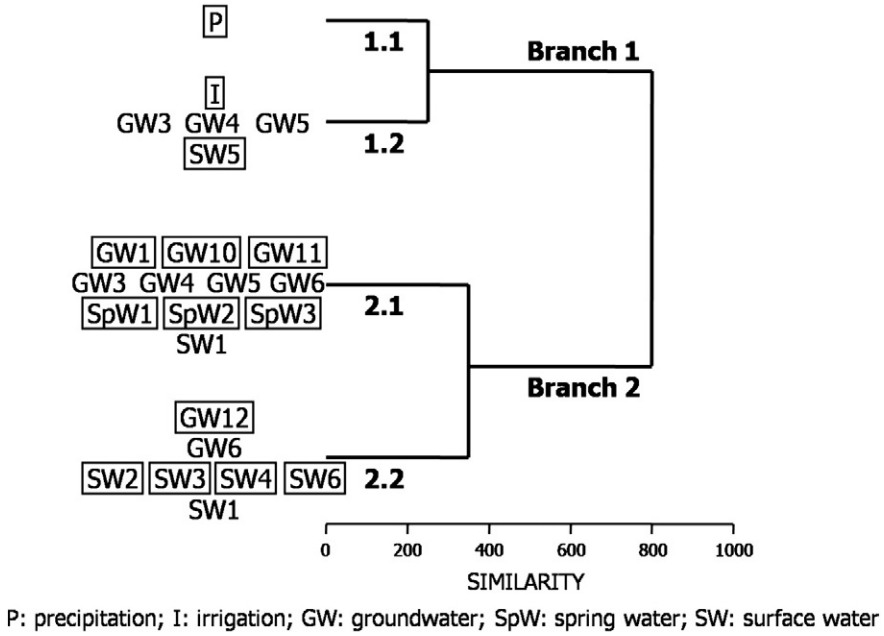

Fig. 8. Simplified results from hierarchical cluster analysis (HCA). For a better visualization, only clustering of similarities above 200 and sampling points (instead of individual samples) are shown. Sampling point names surrounded by a rectangle are the ones for which every single sample falls into the displayed grouping.

The cluster analysis provided several important results regarding the hydrological behavior of the Lerma Basin waters. The existence of irrigation canal seepage was detected by the identification of a surface water location in a group highly influenced by irrigation water. Moreover, high hydrochemical similarity was detected between ground- and spring water, which was in agreement with other observations in the ion–ion ratios or in the statistical comparisons. Groundwaters in some areas of the study zone, mainly southern glacis water body, where the nodular gypsum strata severely affects water quality, presented higher salt contents, providing a higher salinity to the waters in these areas of the basin. This fact is in line with the main hypothesis, which suggests that the geological set up controls the salinization processes in this area.

4.6. Geochemical modeling

4.6.1. Inverse modeling

Taking into account all the feasible mineral phases inferred in the previous sections, mass balance calculations were performed using PHREEQC software. The global uncertainty of analytical results was limited to 5%. The more simplistic models coherent with the observations made in previous sections of the study were selected. The possible processes considered in the mass balance include:

- Evapotranspiration of water with no dissolved content (only in those balances in which the initial water was precipitation or irrigation water).
- Dissolution of halite, gypsum and epsomite.
- Calcite precipitation.
- Dolomite dissolution.
- $CO_2(g)$ exchange.
- Cation exchange.
- NO_3^- sources/sinks.

Mass balance calculations were performed between water samples located in feasible flow lines, i.e., from precipitation and irrigation waters to groundwaters, from ground- to spring waters and from spring to surface waters. This approach assumes that surface water origin is mainly from springs and seepages coming from groundwater, which can be justified since intermittent streams became perennial streams after the implementation of irrigation in the Lerma Basin (Merchán et al., 2013). In most of the flow lines, the results gave the dissolution of either gypsum or epsomite to fit the sulfate concentration in the mass balance (Table 4). When gypsum was used, the addition of Ca^{2+} made necessary that higher amounts of calcite precipitate and dolomite dissolve to fit the concentrations of Ca^{2+} and Mg^{2+}. When epsomite was used, lower calcite precipitation and dolomite dissolution were required. A situation between these two extremes is probably happening in the Lerma Basin waters.

As an example, a flow line in the hydrological system is represented by samples I → GW11 → GW10 → SpW2 → SW3, i.e., irrigation water applied to the crops infiltrates and flows through the glacis until it reaches the Tertiary materials, where it seeps out to the surface. There, it follows a diffuse flow until it reaches the gullies (Fig. 9). Geochemical mass balance results for this flow line are shown in Table 4. The calculations correspond to the data from the sampling campaign on July 27th 2011, during the irrigation season, but they are also representative of those observed in other sampling dates.

According to these results, the groundwater chemical composition (I → GW11 in the example in Table 4) could be explained by the combination of the following processes: evapotranspiration of precipitation or irrigation water, cation exchange, halite and gypsum/epsomite dissolution, $CO_2(g)$ input and dissolution of NO_3^- from fertilizers.

Along the groundwater flow (GW11 → GW10 → SpW2 in the example in Table 4), the net geochemical reactions include the dissolution of small amounts of halite and gypsum/epsomite, and the addition of nitrate leached from agricultural soils. The degasification of $CO_2(g)$-enriched groundwater takes place at the inter-phase between groundwaters and surface waters, which produces the precipitation of calcite.

Finally, when the seeped groundwater reaches the surface drainage network (SpW2 → SW3 in the example in Table 4), the net geochemical reactions include the dissolution of important amounts of halite and gypsum/epsomite, with the consequent precipitation of calcite and dissolution of dolomite. The losses of nitrate are also significant processes in this step.

The mass balance approach supported the processes exposed in the previous sections. Thus, the main geochemical reactions required included: the evapotranspiration of 64%–81% of irrigation water (values in the range of those reported for irrigation efficiency in the study area by Abrahão et al., 2011a, 72%), the addition of $CO_2(g)$ (probably from soil respiration processes, Kehew, 2001), the cation exchange (mainly during the first part of the flow line) and the dissolution of halite and gypsum/epsomite. The dissolution of gypsum triggers the concomitant precipitation of calcite/dissolution of dolomite (e.g., Appelo and Postma, 2005). The enrichment in $CO_2(g)$ produced in soils is partially lost when the groundwater reaches the springs and gets into contact with the atmosphere. Finally, nitrate increases during the whole groundwater flow line and suffers a significant decrease in the surface waters. Merchán et al. (2014), proposed a combination of dilution with upstream waters and denitrification in diffuse surface flow paths as a probable explanation for the lower NO_3^- concentrations observed in surface waters in the Lerma Basin.

4.6.2. Direct modeling

The geochemical evolution of irrigation water was simulated by direct modeling with PHREEQC in order to confirm the main processes detected. The steps followed in this simulation are reported in Fig. 9. The simulations were performed with a fixed saturation index for calcite ($SI_{calcite} = 1.2$) which is around the maximum observed in the Lerma Basin waters. Additional tests were simulated using different

Table 4
Inverse modeling results (PHREEQC) after a mass balance between sampled points in a representative flow line during the irrigation season (July 27th 2011). In mass balances with two columns, results considering either gypsum (a), or both epsomite and gypsum (b), are presented. Positive values means mass entering water, negative values means mass leaving water and no value means no mass transfer.

Phases	I → GW11		GW11 → GW10	GW10 → SpW2	SpW2 → SW3	
(mmol L^{-1})	(a)	(b)			(a)	(b)
Halite			4.85	0.92	9.00	9.01
Gypsum	0.65			0.48	3.87	2.21
Epsomite		0.64				1.66
NaX	1.76	1.74	1.01			
CaX_2	−0.88	−0.87	−0.51			
$CO_2(g)$	0.64	0.65		−1.30	0.78	0.78
Calcite	−1.18	0.00		−0.31	−4.05	−0.73
Dolomite	1.08	0.49	0.43		1.66	0.00
NO_3^-	0.68	0.67	0.84	0.45	−1.61	−1.61
H_2O (mol L^{-1})	−25.20[a]	−25.54[a]				

[a] Implies c.a. 46% evapotranspiration.

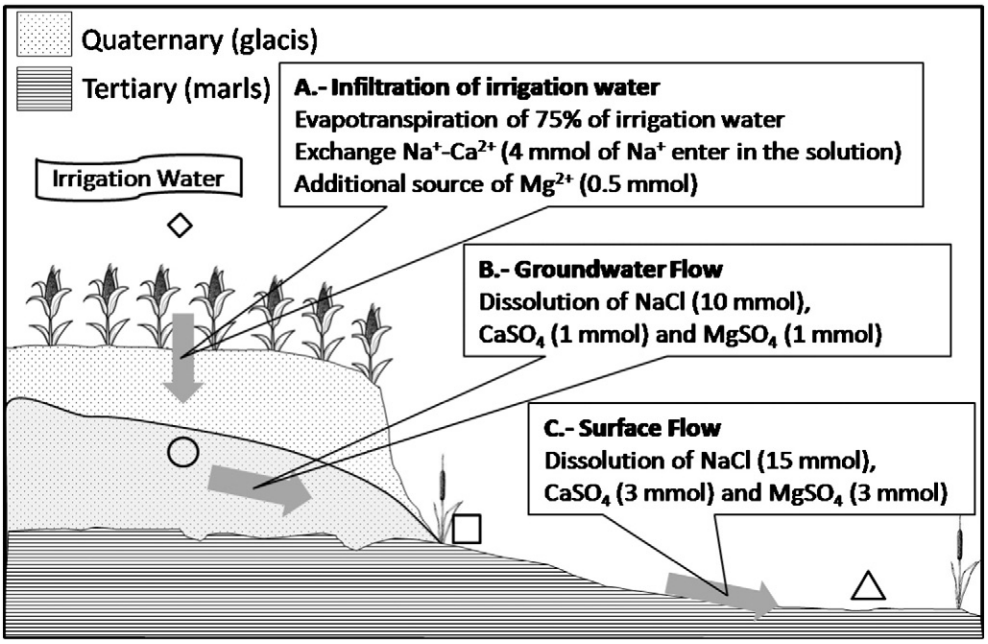

Fig. 9. Conceptual model with performed simulations in the Lerma Basin through PHREEQC. Diamond, circle, square and triangle indicate irrigation, ground, spring and surface waters respectively.

pCO_2 conditions covering the range observed in the Lerma Basin waters ($10^{-2.0}$ and $10^{-2.5}$). The modeling steps start with the infiltration of irrigation water in the aquifer (A, Fig. 9), then the enrichment in salts in groundwater (B, Fig. 9), and finally a higher enrichment in salts during the surface flow (C, Fig. 9). The proportions of solutes have been selected to match the observations from the mass balance results.

The theoretical results of these simulations are included in the previously discussed ionic ratio plots with the real measured data (gray lines in Fig. 5). They indicate that the combination of the processes inferred in previous sections reproduces fairly well the geochemical evolution of the dataset, underpinning confidence in the proposed processes.

Nitrification of non-nitrate fertilizers or denitrification have not been considered in this simulation, although in some studies significant changes in water geochemistry have been reported as a consequence of these processes (e.g., Kim et al., 2005; Koh et al., 2007). However, the fact that a rather good reproduction of the geochemical evolution can be achieved without considering NO_3^- pollution in the geochemical model supports our hypothesis on the independence of the salinization and nitrate pollution processes in this specific study case.

Consequently, our study suggests that the main factor controlling water salinization processes is the geological setup, while the anthropogenic influence seems to play a negligible influence compared to the natural processes. Therefore, the main possible remediation strategies should be linked to an adequate management of irrigation water to decrease the salt loads to downstream waters (Abrahão et al., 2011b; Duncan et al., 2008; García-Garizábal et al., 2009). However, the enrichment in inorganic ions (Na^+, Cl^-, Ca^{2+}, Mg^{2+} and SO_4^{2-}) is not the major component of agricultural pollution. Those components provided exclusively by agricultural pollution, such as NH_4^+, organic carbon or phosphate were not included in this study. Nevertheless, the influence of these other components in water salinity is expected to be negligible.

5. Conclusions

In this work, the geochemical processes affecting water salinization in an irrigated basin were studied through a multidisciplinary approach including laboratory and field data, statistics and modeling. All the information collected pointed to the natural control of salinization processes with non-significant influence of anthropogenic factors.

Among all the soils in the study zone, those developed over the Tertiary materials are the main providers of salts to the waters. The dissolution of halite and gypsum, along with cation exchange, are the main processes that increase water salinity. They generate a significant increase in salinity from recharge (precipitation and irrigation) to discharge water (surface water at the outlet of the basin), with consequent decrease in water quality.

Groundwater is in equilibrium with calcite and dolomite, but highly undersaturated with respect to gypsum and halite. Under these conditions, the dissolution of gypsum probably forces the precipitation of calcite and the concomitant dolomite dissolution. Surface water is oversaturated with respect to both calcite and dolomite, as a consequence of surface water degasification, but still undersaturated with respect to gypsum and halite.

Multivariate analysis suggests independence of the processes controlling water salinization and nitrate pollution, from natural and anthropogenic controls, respectively. Apart from recharge waters, two groups of waters are differentiated: ground- and spring water; and surface waters, with lower and higher salinity, respectively.

Finally, the hypotheses about geochemical reactions and the independence of nitrate pollution and salinization were confirmed through the use of modeling tools, supporting the predominance of natural processes controlling salinization in the Lerma Basin waters.

Acknowledgments

This work was performed within the framework of projects CGL-2009-13410-C02-01 (Spanish Ministry of Economy and Competitiveness) and CGL-2012-32395 (Spanish Ministry of Economy and Competitiveness–FEDER funds [EU]). Daniel Merchán acknowledges the support of grant BES2010-034124, from the same institution. Additionally, this study forms part of the activities of the Geochemical Modelling Group (Aragón Government and University of Zaragoza). Thanks are also due to Geological Survey of Spain and University of Zaragoza for providing equipment and infrastructure. Finally, we acknowledge the valuable help of Eduardo Garrido, Raphael Abrahão and Mónica Blasco (sampling campaigns), Enrique Oliver (lab support) and Begoña del Moral (X-ray diffractions). We also appreciate the thoughtful comments

of three anonymous reviewers, which greatly increased the quality of the manuscript.

References

Abrahão R, Causapé J, García-Garizábal I, Merchán D. Implementing irrigation: water balances and irrigation quality in the Lerma basin (Spain). Agric Water Manag 2011a;102:97–104.

Abrahão R, Causapé J, García-Garizábal I, Merchán D. Implementing irrigation: salt and nitrate exported from the Lerma basin (Spain). Agric Water Manag 2011b;102:105–12.

Acero P, Gutiérrez F, Galve JP, Auqué LF, Carbonel D, Gimeno MJ, et al. Hydrochemical characterization of an evaporite karst area affected by sinkholes (Ebro Valley, NE Spain). Geol Acta 2013;11(4):389–407.

Adams S, Titus R, Pietersen K, Tredoux G, Harris C. Hydrochemical characteristics of aquifers near Sutherland in the Western Karoo, South Africa. J Hydrol 2001;241:91–103.

AEMET (Agencia Estatal de Meteorología). Datos climatológicos (in Spanish). Spain: Gobierno de España, Ministerio de Alimentación, Agricultura y Medio Ambiente. www.aemet.es, 2014. [accessed 2nd July 2014].

Appelo CAJ, Postma D. Geochemistry, groundwater and pollution (2nd edition). The Netherlands: Leiden; 2005. 649 pp.

Ayers RS, Westcot DW. Water quality for agriculture. FAO Irrigation and Drainage Paper No. 29. Rome, Italy: Food and Agriculture Organization of the United Nations; 1992. p. 174.

Beltrán A. Estudio de suelos de la zona regable de Bardenas II. Sectores: VIII, XI, X, XII y XIII. Instituto Nacional de Reforma y Desarrollo Agrario. Spain: Ministerio de Agricultura, Pesca y Alimentación; 1986.

Cameron EM. Hydrogeochemistry of the Fraser River, British Columbia: seasonal variation in major and minor components. J Hydrol 1996;182:209–25.

Carol E, Kruse E, Mas-Pla J. Hydrochemical and isotopical evidence of ground water salinization processes on the coastal plain of Samborombón Bay, Argentina. J Hydrol 2009;365(3–4):335–45.

Carreira PM, Marques JM, Nunes D. Source of groundwater salinity in coastline aquifers based on environmental isotopes (Portugal): natural vs. human interference. A review and reinterpretation. Appl Geochem 2014;41:163–75.

Causapé J, Auqué L, Gimeno MJ, Mandado J, Quílez D, Aragüés R. Irrigation effects on the salinity of the Arba and Riguel Rivers (Spain): present diagnosis and expected evolution using geochemical models. Environ Geol 2004a;45:703–15.

Causapé J, Quílez D, Aragüés R. Assessment of irrigation and environmental quality at the hydrological basin level — I. Irrigation quality. Agric Water Manag 2004b;70:195–209.

Chaudhuri S, Ale S. Long term (1960–2010) trends in groundwater contamination and salinization in the Ogallala aquifer in Texas. J Hydrol 2014;513:376–90.

Davis JC. Statistics and data analysis in geology. New York: Wiley; 1986. 646 p.

Duncan RA, Bethune MG, Thayalakumaran T, Christen EW, McMahon TA. Management of salt mobilisation in the irrigated landscape — a review of selected irrigation regions. J Hydrol 2008;351:238–52.

Edmunds WM. Geochemistry's vital contribution to solving water resource problems. Appl Geochem 2009;24(6):1058–73.

Evans CD, Davies TD, Wigington Jr PJ, Tranter M, Krester WA. Use of factor analysis to investigate processes controlling the chemical composition of four streams in the Adirondack Mountains, New York. J Hydrol 1996;185:297–316.

Fetter Jr CW. Applied hydrogeology. 3rd ed. New York: Prentice-Hall Publishing Co.; 2001. p. 691.

García-Garizábal I, Causapé J, Abrahão R. Evolution of the efficiency and agro-environmental impact of a traditional irrigation land in the middle Ebro Valley (2001–2007). Span J Agric Res 2009;7(2):465–73.

García-Garizábal I, Gimeno MJ, Auqué LF, Causapé J. Salinity contamination response to changes in irrigation management — application of geochemical codes. Span J Agric Res 2014;12(2):376–87.

Hair J, Anderson R, Tatham R, Black W. Análisis Multivariante. Madrid: Prentice Hall Iberia; 1999. 832 pp.

Han D, Song X, Currell MJ, Cao G, Zhang Y, Kang Y. A survey of groundwater levels and hydrogeochemistry in irrigated fields in the Karamay Agricultural Development Area, northwest China: implications for soil and groundwater salinity resulting from surface water transfer for irrigation. J Hydrol 2011;405(3–4):217–34.

Helsel DR, Hirsch RM. Statistical methods in water resources. Techniques of water resources investigations, Book 4, Chapter A3. Reston, VA: US Geological Survey; 2002. p. 510.

Isidoro D, Quílez D, Aragüés R. Environmental impact of irrigation in La Violada District (Spain): I. Salt export patterns. J Environ Qual 2006;35:766–75.

ITGE. Mapa geológico de España. Ejea de los caballeros (map and memory). No. 284 27-12. Madrid: Instituto Tecnológico Geominero de España; 1988.

Jalali M. Assessment of the chemical components of Fameningroundwater, western Iran. Environ Geochem Health 2005;29:357–74.

Jalali M. Major ion chemistry of groundwaters in the Bahar area, Hamadan, western Iran. Environ Geol 2007;47:763–72.

Johansson O, Aimbetov I, Jarsjö J. Variation of groundwater salinity in the partially irrigated Amudarya River delta, Uzbekistan. J Mar Syst 2009;76(3):287–95.

Kehew AE. Applied chemical hydrogeology. Prentice Hall Inc.; 2001 [368 pp.].

Kelly WP. Use of saline irrigation water. Soil Sci 1963;95:385–91.

Kim K, Rajmohan N, Kim H-J, Kim S-H, Hwang G-S, Yun S-T, et al. Evaluation of geochemical processes affecting groundwater chemistry based on mass balance approach: a case study in Namwon, Korea. Geochem J 2005;39:357–69.

Koh D-C, Ko K-S, Kim Y, Lee S-G, Chang H-W. Effect of agricultural land use on the chemistry of groundwater from basaltic aquifers, Jeju Island, South Korea. Hydrogeol J 2007;15:727–43.

Kume T, Akca E, Nakano T, Nagano T, Kapur S, Watanabe T. Seasonal changes of fertilizer impacts on agricultural drainage in a salinized area in Adana, Turkey. Sci Total Environ 2007;408:3319–26.

Langmuir D, Melchior D. The geochemistry of Ca, Sr, Ba and Ra sulfates in some deep brines from the Paulo Duro Basin, Texas. Geochim Cosmochim Acta 1985;49:2423–32.

Li X-D, Masuda H, Kusakabe M, Yanagisawa F, Zeng H-A. Degradation of groundwater quality due to anthropogenic sulfur and nitrogen contamination in the Sichuan Basin, China. Geochem J 2006;40:309–32.

Lorite-Herrera M, Jiménez-Espinosa R, Jiménez-Millán J, Hiscock KM. Integrated hydrochemical assessment of the Quaternary alluvial aquifer of the Guadalquivir River, southern Spain. Appl Geochem 2008;23:2040–50.

Menció A, Folch A, Mas-Pla J. Identifying key parameters to differentiate groundwater flow systems using multifactorial analysis. J Hydrol 2012;472–473:301–13.

Merchán D, Causapé J, Abrahão R. Impact of irrigation implementation on hydrology and water quality in a small agricultural basin in Spain. Hydrol Sci J 2013;58(7):1400–13.

Merchán D, Otero N, Soler A, Causapé J. Main sources and processes affecting dissolved sulphates and nitrates in a small irrigated basin (Lerma Basin, Zaragoza, Spain): isotopic characterization. Agric Ecosyst Environ 2014;195:127–38.

Morán-Tejeda E, López-Moreno JI, Ceballos-Barbancho A, Vicente-Serrano SM. River regimes and recent hydrological changes in the Duero basin (Spain). J Hydrol 2011;404:241–58.

Moussa AB, Zouari K, Marc V. Hydrochemical and isotope evidence of groundwater salinization processes on the coastal plain of Hammamet-Nabeul, north-eastern Tunisia. Phys Chem Earth 2011;36:167–78.

Nakano T, Tayasu I, Yamada Y, Hosono T, Igeta A, Hyodo F, et al. Effect of agriculture on water quality of Lake Biwa tributaries, Japan. Sci Total Environ 2008;389:132–48.

Nielsen DL, Brock MA, Rees GN, Baldwin DS. Effects of increasing salinity on freshwater ecosystems in Australia. Aust J Bot 2003;51:655–65.

Otero N, Vitòria L, Soler A, Canals A. Fertiliser characterization: major, trace and rare earth elements. Appl Geochem 2005;20:1473–88.

Parkhurst DL, Appelo CAJ. User's guide to PHREEQC (version 2.0) — a computer program for speciation, batch-reaction, one-dimensional transport, and inverse geochemical calculations. Water-resources investigations report 99-4259. Denver, Colorado, USA: US Geological Survey; 1999. p. 326.

Peck AJ, Hatton T. Salinity and the discharge of salts from catchments in Australia. J Hydrol 2003;272:191–202.

Plummer N, Busby J, Lee R, Hanshaw B. Geochemical modelling of the Madison aquifer in parts of Montana, Wyoming, and South Dakota. Water Resour Res 1990;26:1981–2014.

Richter BC, Kreitler CW. Identification of sources of ground-water salinization using geochemical techniques. Oklahoma: U.S. Environmental Protection Agency. Ada; 1991. 273 pp.

Sánchez D, Vadillo I, Carrasco F, Mancera E. Contamination by agricultural-origin nitrogen compounds within a porous multilayer aquifer in southern Spain. In: Candela L, Vadillo I, Aagaard P, Bedbur E, Trevisan M, Vanclooster M, Viotti P, López-Geta JA, editors. Water pollution in natural porous media at different scales. Assessment of fate, impact and indicators. Instituto Geológico y Minero de España; 2007.

Soil Survey Staff. Keys to soil taxonomy. 12th ed. United States Department of Agriculture — Natural Resources Conservation Service; 2014.

Statpoint Technologies. Statgraphics Centurion XVI. User manual. StatPoint Technologies Inc.; 2009. p. 297.

Stigter TY, Carvalho-Dill AMM, Ribeiro L, Reis E. Impact of the shift from groundwater to surface water irrigation on aquifer dynamics and hydrochemistry in a semi-arid region in the south of Portugal. Agric Water Manag 2006;85:121–32.

Tanji K. Agricultural salinity assessment and management. Am Soc Civ Eng 1990;71:619.

Tedeschi A, Beltrán A, Aragüés R. Irrigation management and hydrosalinity balance in a semi-arid area of the middle Ebro river basin (Spain). Agric Water Manag 2001;49:31–50.

van Asten PJA, Barbiéro L, Wopereis MCS, Maeght JL, van der Zee SEATM. Actual and potential salt-related soil degradation in an irrigated rice scheme in the Sahelian zone of Mauritania. Agric Water Manag 2003;60(1):13–32.

Weight WD. Hydrogeology field manual. 2nd ed. USA: McGraw-Hill Companies Inc.; 2008. p. 751.

Yuce G, Pinarbasi A, Ozcelik S, Ugurluoglu D. Soil and water pollution derived from anthropogenic activities in the Porsuk River Basin, Turkey. Environ Geol 2006;49:359–75.

Zhu C, Anderson G. Environmental applications of geochemical modeling. Cambridge University Press; 2002. p. 284.